

COVERS ~~UNSAT SOIL~~

Hydrologic Modeling of Protective Barriers: Comparison of Field Data and Simulation Results

M. J. Fayer,* M. L. Rockhold, and M. D. Campbell

ABSTRACT

Protective barriers, which consist of layers of silt loam over sand and gravel, have been proposed as covers for waste sites located in semiarid south-central Washington state. The ability of an uncalibrated model to predict water contents, water storage, and drainage in barriers was tested for durations as long as 1.5 yr. Eight nonvegetated lysimeters containing the barrier layering sequence have been monitored since November 1987. The lysimeters were subjected to one of three precipitation treatments: ambient, 2× average, and breakthrough (i.e., until drainage occurred). Distributions of measured and simulated water contents with depth were similar; maximum differences ranged from 0.023 cm³/cm³ for the ambient treatment to 0.089 cm³/cm³ near the soil-sand interface for the breakthrough treatment. Simulated storage followed the trend in the measured values, although differences as much as 5 cm were observed at certain times. Generally, the model overpredicted evaporation in the winter and underpredicted it in the summer. Root-mean-square errors were 1.47 and 2.21 cm for the ambient and 2×-average treatments, respectively. Sensitivity tests revealed that the hydraulic-conductivity function, snow cover, and potential evaporation were important to successful modeling of storage in a protective barrier. When the above parameters and processes were adjusted (though not optimized), the root-mean-square error for the 2×-average treatment was reduced 63% to 0.81 cm. For the breakthrough treatment, simulated drainage was obtained only by using field-measured sorption and saturated-conductivity data. This result indicates that hysteresis is important to successful modeling of drainage through protective barriers.

RADIOACTIVE WASTE has been disposed at a variety of locations at the U.S. Department of Energy's Hanford Site in semiarid south-central Washington state, using methods such as subsurface tanks, burial of solid waste, and direct application of liquids to the sediments. Some of these waste-disposal sites need to be isolated from infiltrating water to minimize the potential for transport of contaminants from the waste to the unconfined aquifer, which eventually discharges into the Columbia River. Multilayer protective barriers have been proposed as a means of limiting the flow of water through the waste sites (U.S. Department of Energy, 1987).

A protective barrier consists of layers of fine-textured soil overlying coarser textured soil. The textural contrast delays the drainage of water from the upper layer when it is unsaturated, thus lengthening the duration of time during which the stored water could be evaporated or used by plants (Miller, 1971). A multiyear research program was designed to assess the ability of these barriers to reduce drainage rates to the deeper vadose zone to <0.05 cm/yr. One aspect of this program is to develop computer models to predict the barrier's water balance, of which drainage is one component.

Earth & Environmental Science Dept.
Geosciences Dep., Pacific Northwest Lab., P.O. Box 999, Richland, WA 99352. Prepared for the U.S. Dep. of Energy under Contract DE-AC06-76 RLO 1830. Received 7 May 1990. *Corresponding author.

Published in Soil Sci. Soc. Am. J. 56:690-700 (1992)

Traditionally, water-balance models have been evaluated for durations ranging from days to months for agricultural or remote-sensing purposes (e.g., Lascano et al., 1987; Sellers and Dorman, 1987; Horton, 1989; Witono and Bruckler, 1989). To our knowledge, few studies have focused on the water balance of nonirrigated waste-disposal sites in a semiarid climate for durations in excess of several consecutive months. The primary objective of this study was to assess the ability of the UNSAT-H Version 2.0 model (Fayer and Jones, 1990) to simulate the water balance of the protective barrier for durations in excess of a year without prior calibration of the model parameters. A secondary objective was to collect information that could be used to improve the water-balance model, thus allowing for better predictions of long-term drainage rates through the barrier.

MODEL DESCRIPTION

The model UNSAT-H, Version 2.0, is a one-dimensional unsaturated soil-water and heat-flow model. Because we are still testing the heat-flow component and did not initially have detailed information on thermal processes affecting evaporation at our lysimeter site, we performed the simulations without directly including heat flow.

The flow of water is calculated using Richards' equation for liquid water flow in response to gravitational and suction-head gradients and Fick's law for diffusive vapor flow. The water-flow equation is

$$C(h)\partial h/\partial t = -\partial/\partial z [K_T(h)\partial h/\partial z + K_L(h) + q_{vT}] - S(z,t) \quad [1]$$

- where $C = \partial\theta/\partial h$, the negative of the specific water capacity (1/cm)
 θ = volumetric water content (cm³/cm³)
 h = suction head, the negative of the soil water pressure head (cm)
 t = time (h)
 z = depth below the soil surface (cm)
 $K_T = K_L + K_{vh}$
 K_L = liquid water conductivity (cm/h)
 K_{vh} = vapor conductivity relative to a suction-head gradient (cm/h)
 q_{vT} = vapor flux induced by a thermal gradient (cm/h)
 S = sink term for water uptake by plants (1/h)

For this study, soil temperature was maintained constant so that q_{vT} was zero because heat flow was not considered, and S was not needed because the model applications were for protective barriers without vegetation.

The derivation of K_{vh} described by Simmons and Gee (1981) is presented here for clarity. The derivation begins with a form of Fick's law of diffusion (Hillel, 1980), which can be written as

$$q_v = -(D/\rho_w) \partial \rho_v/\partial z \quad [2]$$

- where q_v = flux of water vapor (cm/h)
 ρ_w = density of liquid water (g/cm³)
 D = diffusion coefficient for water vapor in soil (cm²/h)
 ρ_v = vapor density (g/cm³)

The diffusion coefficient accounts for the tortuosity of the diffusion path and the reduced cross-sectional area for flow via the relationship

$$D = \alpha(\theta_s - \theta)D_a \quad [3]$$

where α is the tortuosity factor, D_a is the diffusivity of water vapor in bulk air (cm^2/h), and the quantity $(\theta_s - \theta)$ represents the air-filled porosity (cm^3/cm^3). Differentiating Eq. [2] to explicitly include gradients for suction head and temperature produces

$$q_v = -(D/\rho_w)(\partial\rho_v/\partial h)\partial h/\partial z - (D/\rho_w)(\partial\rho_v/\partial T)\partial T/\partial z \quad [4]$$

where T is the temperature (K). The two terms on the right-hand side of Eq. [4] are the isothermal and thermal vapor fluxes, q_{vh} and q_{vT} , respectively. Under isothermal conditions, q_{vT} equals zero and the total vapor flux equals q_{vh} . The vapor density at a specific point in the soil is related to the saturated vapor density, ρ_{vs} , and relative humidity, RH, by

$$\rho_v = \rho_{vs}RH \quad [5]$$

The relative humidity is determined using

$$RH = \exp(-hMg/RT) \quad [6]$$

where M is the molecular weight of water (g/mol), g the gravitational constant (cm/s^2), the R the gas constant (erg/mol/K). Combining Eq. [4], [5], and [6] for an isothermal system and rearranging yields

$$q_{vh} = (D/\rho_w)\rho_{vs}(Mg/RT)RH(\partial h/\partial z) \quad [7]$$

Equation [7] is similar to the flux equation for liquid flow. As such, most of the parameters can be combined to yield the isothermal vapor-conductivity term

$$K_{vh} = (D\rho_{vs}Mg/\rho_wRT)RH \quad [8]$$

that is used in Eq. [1].

The flow equation is discretized using a Crank-Nicolson finite-difference scheme similar to that used by Nimah and Hanks (1973). The discretized equations are solved for a given time step using the Thomas algorithm (Wang and Anderson, 1982). The size of the time step can vary between defined minimum and maximum values; the actual size depends on the magnitude of the mass-balance error relative to the allowable error.

For this study, infiltration was described as a flux of either precipitation or irrigation, with no runoff. Evaporation was described as either a flux or fixed-head condition (Gupta et al., 1978). The condition depends on the value of h_s , the suction head at the surface node, relative to the limit, h_{max} . If $h_s < h_{max}$, evaporation is set equal to the potential evaporation rate, which is calculated from meteorologic parameters. If h_s is predicted to be $> h_{max}$ at the end of a time step, that particular time step is repeated with the h_s prediction fixed at the value of h_{max} , i.e., a fixed-head condition. The evaporation rate is then a function of the net flux to the surface node from the node below. During this stage, the soil conductivity significantly affects the evaporation rate.

METHOD

The method used to document the ability of UNSAT-H Version 2.0 to predict the water balance of eight nonvegetated lysimeters, located in the Field Lysimeter Test Facility described by Gee et al. (1989), was to compare the simulation results (i.e., water contents, storage, and drainage) with measurements. Although they are an integral part of the protective barrier, plants were not included in this

analysis in order to simplify testing of the other components of the model.

None of the parameters used in the simulations reported here were calibrated. Instead, the parameters were determined independent of the simulations using standard methods to illustrate how well the model could perform without calibration.

Six of the eight lysimeters were cylinders with bottoms that were sealed except for a drain (Fig. 1a). These drainage lysimeters comprised two replicates of three precipitation treatments: ambient (i.e., natural precipitation), $2\times$ average (water added to achieve twice the average precipitation received from 1955 to 1980), and breakthrough (i.e., water added until drainage occurred).

The remaining two lysimeters were rectangular parallelepipeds, 152 cm on the sides and 170 cm high. The bottoms were sealed except for a drain. These lysimeters contained the layering sequence shown in Fig. 1a, except that the lowest layer was the 0.01-m-diam. gravel. These lysimeters rested on platform scales; hence, their designation as weighing lysimeters. Calibration of the scales indicated an accuracy of ± 0.03 cm when measuring storage changes. The weighing lysimeters were replicates of the ambient and $2\times$ average treatments.

The water contents of the lysimeters were monitored biweekly with a neutron probe. Based on calibration data, the accuracy of the probe is ± 0.01 cm^3/cm^3 . The lysimeters were also monitored biweekly for drainage. Collected drainage water was weighed to the nearest gram and expressed as volume per surface area of the lysimeters.

Table 1 lists the lysimeter descriptions, identifiers, and simulation periods for each treatment. Lysimeters D9 and D11 were covered on 14 Mar. 1988 to eliminate evaporation and promote breakthrough. Subsequent weekly irrigations eventually saturated the silt loam; as a result, the soil surfaces subsided approximately 10 cm sometime in July 1988. Therefore, we chose to simulate the water balance of these lysimeters for the period ending 30 June 1988 rather than 30 Apr. 1989 as was done for the other lysimeters.

Barrier Representation

In the conceptual model of the drainage lysimeters (Fig. 1b), the two sand layers were treated as a single sand layer and the various gravel sizes were treated as gravel with an average diameter of 0.01 m. The bottoms of the lysimeters have a slope of 0.02 m/m from the 2.89-m depth to the drain located at 2.93 m. The simulations were made using a uniform depth of 2.93 m and assuming that the slight slope at the bottom would have a negligible effect on the annual flow of water. Trial and error was used to determine the minimum node spacing needed to produce acceptable results yet minimize the required computer time. The chosen spacing for the simulation nodes (Fig. 1b) ranged from 0.2 cm at the surface, to 2.0 cm at material interfaces, to a high of 25 cm in the middle of the gravel. Reducing the node spacing further did not change the simulation results appreciably except for the breakthrough treatment, for which the spacing in the gravel was reduced to 2 cm.

The conceptual model of the two weighing lysimeters is identical to that of the drainage lysimeters, except that the bottom of the weighing lysimeters is at 165 cm rather than at 293 cm. Therefore, below 153 cm, the node spacing is uniformly 2 cm down to 165 cm, which represents the bottom of the weighing lysimeter. For all simulations, node depths within the silt loam layer were the same.

Soil Properties

The silt loam material was excavated from a 5-m-thick sediment deposit located about 10 km west of the lysimeter

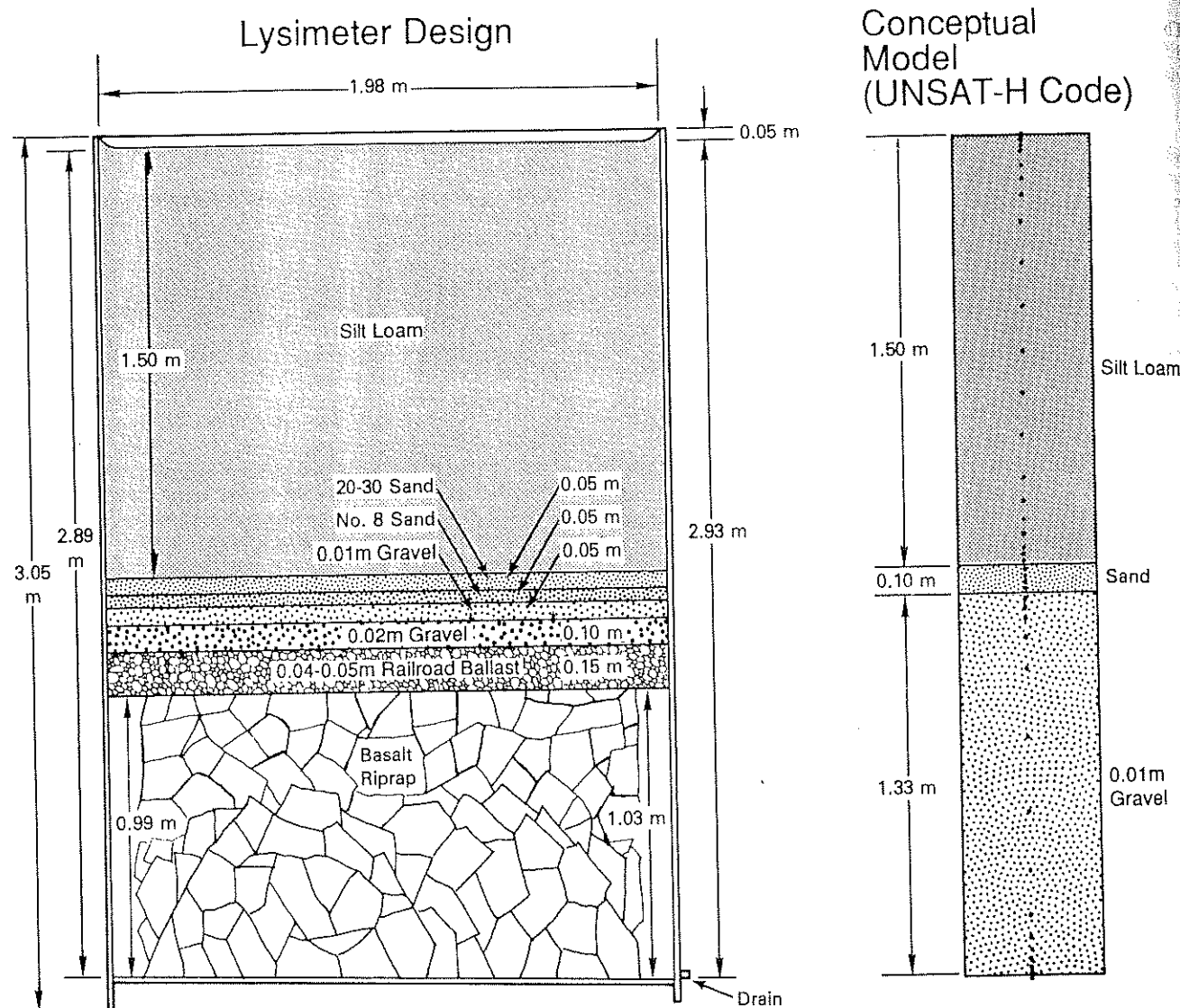


Fig. 1. (a) Lysimeter design and (b) conceptual model used to compare measured and simulated hydrology.

facility. The weathered portions of the sediments are generally classified as coarse-silty, mixed, mesic Xerollic Camborthids. The sands are commercially available materials. More than 90% of the particles of no. 8 sand fall between sieve sizes of 1 and 2 mm. More than 90% of the particles of 20/30 sand fall between sieve sizes of 0.25 and 1.0 mm.

Soil water retention was described using the van Genuchten (1978) model

$$\theta = \theta_r + (\theta_s - \theta_r)[1 + (\alpha h)^n]^{-m} \quad [9]$$

where the subscripts s and r refer to the saturated and residual values and α , n , and m are curve-fitting parameters. The parameter m was assumed to equal $1 - 1/n$. Hydraulic

Table 1. Lysimeter descriptions, identifiers (ID), and simulation periods for each treatment.

Treatment description	Lysimeter ID		Simulation periods	
	Drainage	Weighing	Beginning	End
Ambient	D1, D8	W2	5 Nov. 1987	30 Apr. 1989
2x average	D10, D12	W4	5 Nov. 1987	30 Apr. 1989
Breakthrough	D9, D11	-	5 Nov. 1987	30 June 1988

conductivity was described using Eq. [9] and the Mualem conductivity model (1976a):

$$K = K_s \{1 - (\alpha h)^{n-1} [1 + (\alpha h)^n]^{-m}\}^2 [1 + (\alpha h)^n]^{-cm} \quad [10]$$

where K_s is the saturated conductivity (cm/h) and ℓ is the pore interaction term (dimensionless), which was assumed to be 0.5.

The silt loam parameters were fitted to laboratory desorption data determined for this soil using the hanging water column, pressure plate, and vapor adsorption methods (Gee et al., 1989). The predicted conductivities agreed reasonably with values measured in the suction-head range from 0 to 200 cm using the steady-state flux control method (Klute and Dirksen, 1986).

Hydraulic data for the sand and gravel were unavailable. Because preliminary simulations revealed that the model was relatively insensitive to their hydraulic properties, we described the sand and gravel using proxy data. Sand parameters were fitted to a combination of retention and conductivity data for two sand separates that were numbered 4141 and 4142 in Mualem (1976b). The particle sizes of the sand separates ranged from 0.5 to 1.0 mm and 0.25 to 0.5 mm in diameter, respectively. The gravel parameters

were fitted to the estimated gravel properties reported by Fayer et al. (1985), whose predicted gravel conductivities were similar to measured values reported by Miller and Burger (1963). All fitting was conducted with the RETC computer program (van Genuchten, 1985).

The parameters used to describe the desorption properties of each material are listed in Table 2. Unless noted, all simulations were conducted with these desorption properties. Included in Table 2 are sorption parameters for the silt loam. These parameters were determined using a set of retention data that were collected as lysimeters D9 and D11 were wetting until breakthrough occurred. All of the hydraulic-property functions are shown in Fig. 2. In the simulations, values for internodal conductivities were calculated using the geometric mean.

Initial Conditions

The lysimeters were filled (Fig. 1a) during June 1987 and covered with plastic until 4 Nov. 1987. November 5 was the first simulated day.

The initial water contents of nodes representing the silt loam layer in each lysimeter were derived from neutron-probe readings taken on 4 Nov. 1987 at 15-cm depth intervals from 15 to 135 cm below the soil surface. Water contents above the 15-cm depth were set equal to the neutron-probe reading at the 15-cm depth. Water contents below the 135-cm depth were set equal to the neutron-probe reading at the 135-cm depth. Measurement error above 15 cm and below 135 cm was considered negligible because the water-content profiles measured between these two depths were fairly uniform and the surface of the lysimeters had been covered, preventing significant drying of the surface.

Water contents for nodes located between any two neutron-probe readings were linearly interpolated. Given the initial water content at each node, the initial suction-head value (relative to atmospheric datum) was determined using the soil water-retention curves (Fig. 2a).

Water contents were not measured in the sand and gravel layers. To assign initial conditions for these layers, we simulated the redistribution of water in the lysimeters from early June 1987, when the sand and gravel layers were saturated and drained, till 4 Nov. 1987. Initial water contents for all eight lysimeters are shown in Fig. 3.

Boundary Conditions

For modeling purposes, the two boundaries requiring specification were the bottom of the lysimeters and the soil surface. The bottom of the drainage lysimeters was 1.4 m below the silt loam layer. This distance was judged sufficient to represent this boundary as a unit gradient. In con-

trast, the bottom of the weighing lysimeters was only 0.2 m below the silt loam layer, too close to use a unit-gradient boundary. Therefore, the bottom boundary of the weighing lysimeters was represented as a zero-flux condition. This condition was appropriate for the weighing lysimeters because the simulated suction head of the bottom node never decreased to near zero, a condition necessary for drainage to occur.

The boundary at the soil surface was a function of the weather and irrigation treatment. The source of the weather data was the Hanford Meteorological Station (Stone et al., 1983), about 200 m west of the lysimeter facility. Hourly precipitation data were used in the simulations (snow was assumed to melt immediately). In addition to natural precipitation, Columbia River water was added to the 2×-average and breakthrough treatments using a sprinkler irrigation device. The device consisted of a spray bar with six nozzles mounted on a carriage assembly that moved back and forth over the lysimeters. The nozzles dispersed water in a long, narrow elliptical pattern on the soil surface with 50% overlap (Gee et al., 1989). The addition of water was started at 0700 h on the day of application at a rate (nominally 0.4 cm/h) less than the saturated conductivity. Cumulative precipitation for each of the three precipitation treatments is displayed in Fig. 4. The lysimeter design prevented runoff; thus, all precipitation and irrigation infiltrated.

Daily averages of the hourly meteorological data were converted to daily potential evaporation (PE) values using the Penman equation in Doorenbos and Pruitt (1977, p. 1-144). For the time when lysimeters D9 and D11 were covered (i.e., starting on 14 Mar. 1988), the PE values were set to zero so that no evaporation occurred. Cumulative PE

Table 2. Parameters describing the hydraulic properties of materials in the lysimeters with the van Genuchten and Mualem functions.

Material	Parameter†				
	θ_r	θ_s	α	n	K_s
	cm ³ /cm ³	cm ³ /cm ³	1/cm		cm/h
Silt loam					
Laboratory desorption	0.00	0.496	0.0178	1.34	4.03‡
Field sorption	0.00	0.411	0.0419	1.29	3.24§
Sand	0.010	0.445	0.0726	2.80	394.0
Gravel	0.005	0.419	4.93	2.19	1260.0

† θ_r = residual volumetric water content, θ_s = saturated volumetric water content, α and n = curve-fitting parameters, and K_s = saturated hydraulic conductivity.

‡ Fitted value of saturated conductivity.

§ Average of values determined in the field with a Guelph permeameter (Rockhold et al., 1988).

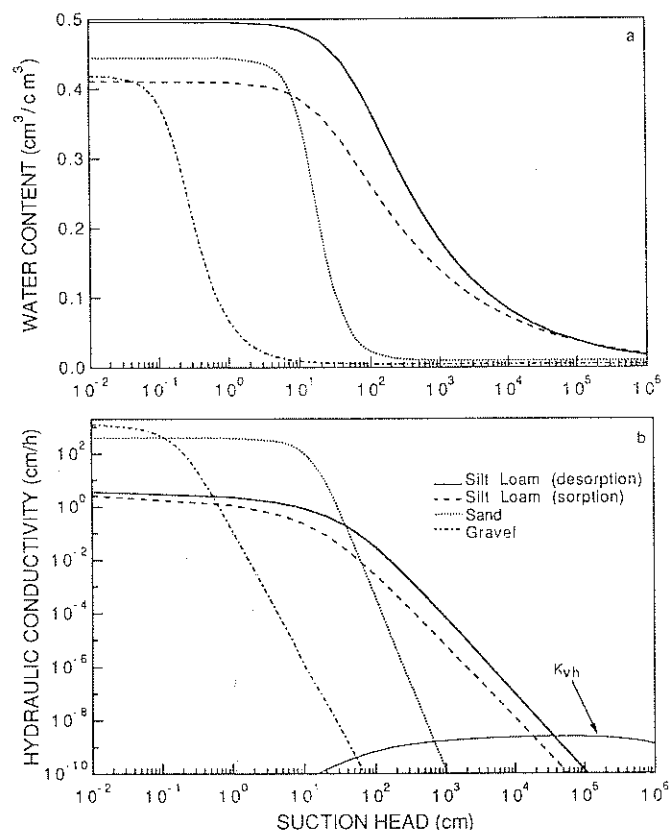


Fig. 2. (a) Water retention and (b) hydraulic conductivity of the materials in the lysimeters. The values of vapor conductivity relative to a suction-head gradient for the silt loam at 15.3 °C are included for comparison.

Exactly what

Not
condition
-ing

A

why

C

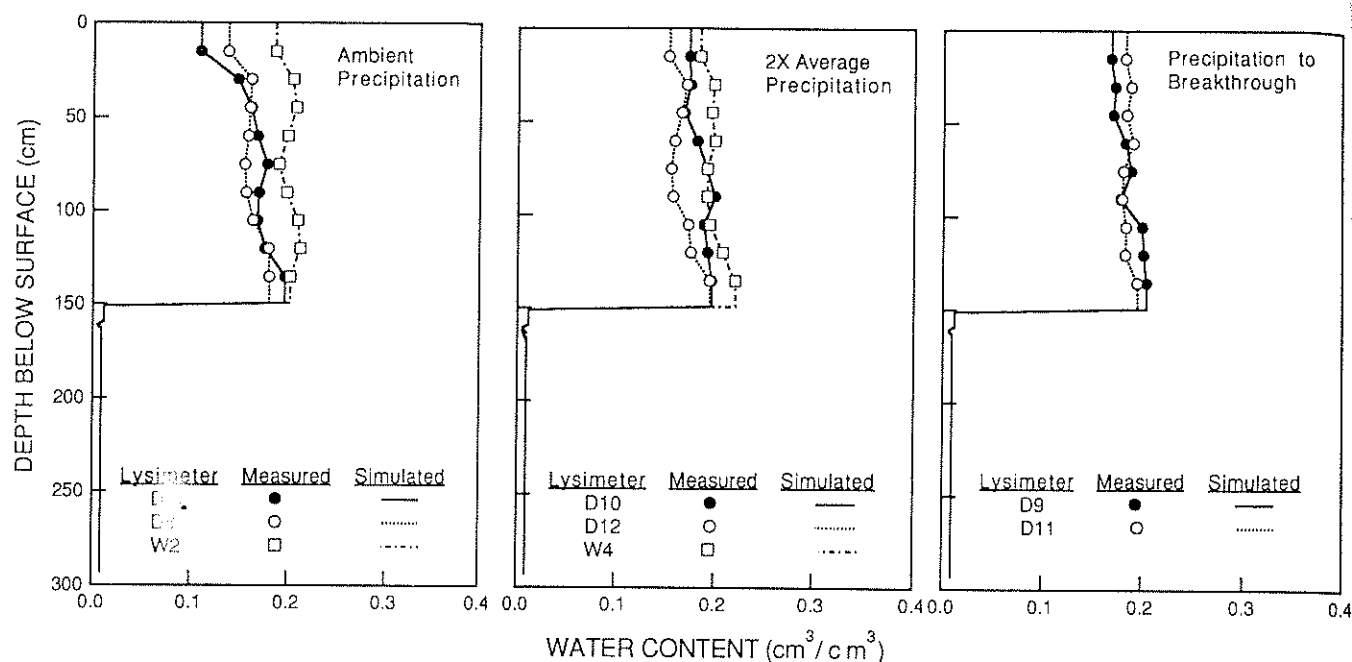


Fig. 3. Initial water contents of all lysimeters for the three precipitation treatments.

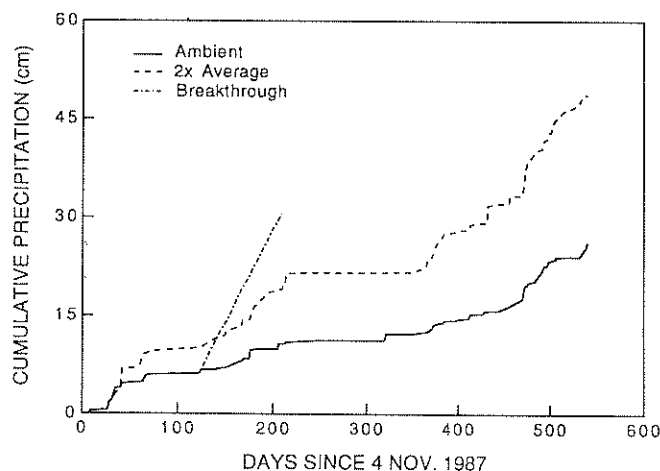


Fig. 4. Cumulative measured precipitation for each of the three precipitation treatments for the durations simulated.

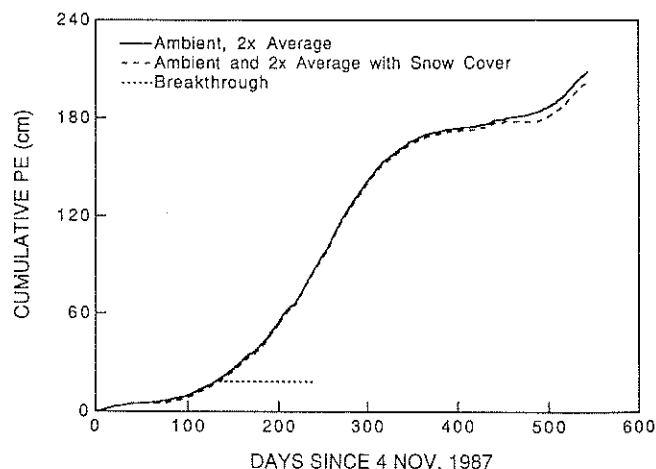


Fig. 5. Cumulative calculated potential evaporation for each of the three precipitation treatments for the durations simulated.

is displayed in Fig. 5 for the ambient and 2 \times -average precipitation treatments, with and without a snow cover (explained below), and for the precipitation to breakthrough treatment.

The daily PE value was distributed throughout the 24 h of the day in the following manner. For the hours from 0600 to 1800, 88% of the daily PE value was assigned in proportion to the average annual receipt of solar radiation during each of those hours. For the 12 night hours, the remaining 12% of the daily PE value was distributed evenly. The maximum suction head (h_{\max}) was specified as 10^6 cm of water.

Simulation Controls

The maximum size of the time steps was specified as 1.0 h to match the hourly precipitation data. Time steps were permitted to vary between 10^{-8} and 1.0 h, depending on the mass-balance error (for more details, refer to the model documentation in Fayer and Jones, 1990). On average, the

simulations required 44 steps per day. The majority of days required only 24 steps; days with precipitation required as many as 350 steps.

RESULTS AND DISCUSSION

Ambient Precipitation Treatment

On 2 Nov. 1988, the measured water-content profiles were the driest since the lysimeters were installed. Following that date, the measured profiles were the wettest on 14 Mar. 1989. Except for the upper 50 cm of the profile on 14 Mar. 1989, the simulated water contents on these dates were within $0.023 \text{ cm}^3/\text{cm}^3$ of the measured values (Fig. 6). On 14 Mar. 1989, the simulations show a pulse of water that was smaller and higher in the profile than measured.

At each depth among the three lysimeters, the sim-

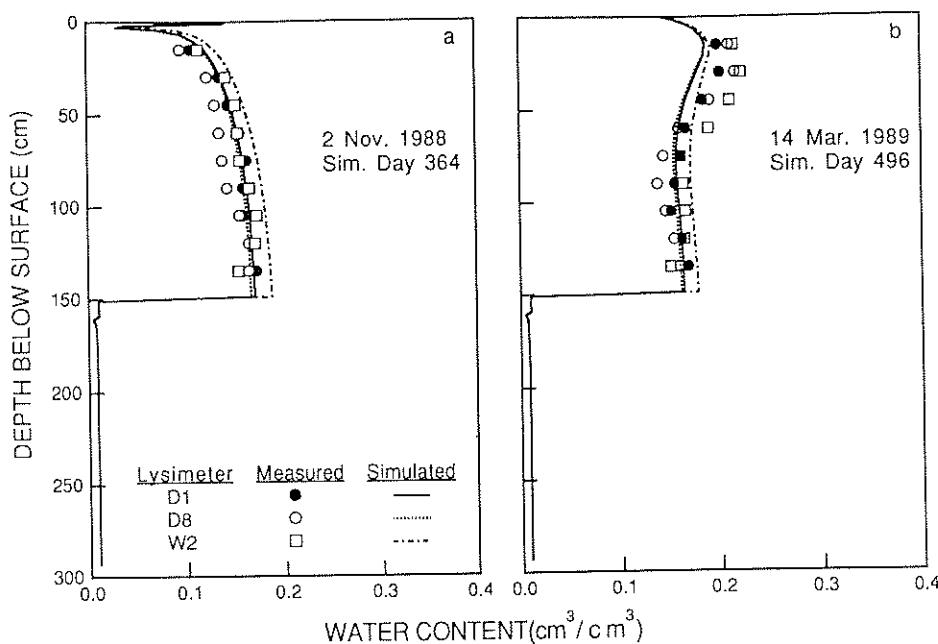


Fig. 6. Measured and simulated water contents for the ambient precipitation treatment on (a) 2 Nov. 1988 and (b) 14 Mar. 1989.

ulated water contents on 14 Mar. 1989 were within $0.015 \text{ cm}^3/\text{cm}^3$ of each other, despite initial differences as large as $0.076 \text{ cm}^3/\text{cm}^3$. At the soil-sand interface, the simulated flux was upward during the entire simulation period. No measurable drainage occurred from these lysimeters.

Figure 7 shows that, during both winters, storage increased, whereas during the summer storage decreased. This pattern is typical of the Hanford Site, which receives 52% of its precipitation in the months of November through February, and 40% of that in the form of snow. Compared with the measured changes, the simulated storage changes were less during all seasons. This result indicates that more evaporation is simulated in the winter and less evaporation during the remainder of the year than actually occurs. A comparison of predicted vs. measured daily storage values yielded a root-mean-square error of 1.47 cm.

Twice-Average Precipitation Treatment

Figure 8 shows that the simulated water contents on 2 Nov. 1988 were as much as $0.038 \text{ cm}^3/\text{cm}^3$ higher than measured, whereas, on 14 Mar. 1989, most of the simulated water contents were as much as $0.045 \text{ cm}^3/\text{cm}^3$ lower than measured. Immediately above the soil-sand interface, simulated water contents were as much as $0.067 \text{ cm}^3/\text{cm}^3$ less than measured.

At each depth among the three lysimeters, the simulated water contents on 14 Mar. 1989 were within $0.015 \text{ cm}^3/\text{cm}^3$ of each other, despite initial differences as large as $0.040 \text{ cm}^3/\text{cm}^3$. The simulated flux at the soil-sand interface was upward until 7 Jan. 1989. After that date, the downward flux into the sand reached its highest value ($0.0087 \text{ cm}/\text{yr}$) on 11 Mar. 1989. The simulated flux at the sand-gravel interface was upward at all times. Similar to the ambient treatment, no measurable drainage occurred from these lysimeters.

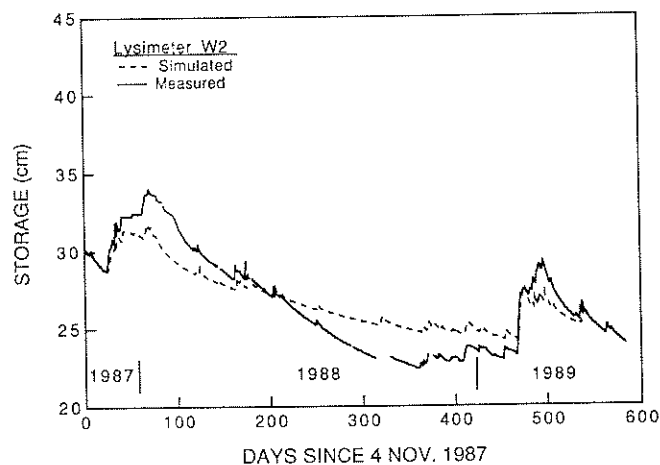


Fig. 7. Measured and simulated storage for the ambient precipitation treatment, lysimeter W2.

Similar to the ambient treatment, measured storage increased during both winters and decreased during the summer, and the simulated storage changes were smaller than the measured changes throughout the simulated period (Fig. 9). This result provides additional evidence that UNSAT-H is simulating more evaporation in the winter and less during the remainder of the year than actually occurs. A comparison of predicted vs. measured daily storage values yielded a root-mean-square error of 2.21 cm.

Additional simulations of lysimeter W4 were conducted to ascertain model sensitivities that might explain the difference between measured and simulated storage. In separate simulations, the value of h_{max} was set to 15,300 cm, historically known as the wilting point for plants, and calculated each day as a function of the mean daily air temperature and vapor density. Neither change resulted in a storage difference >0.5

Handwritten note: 15,300 cm

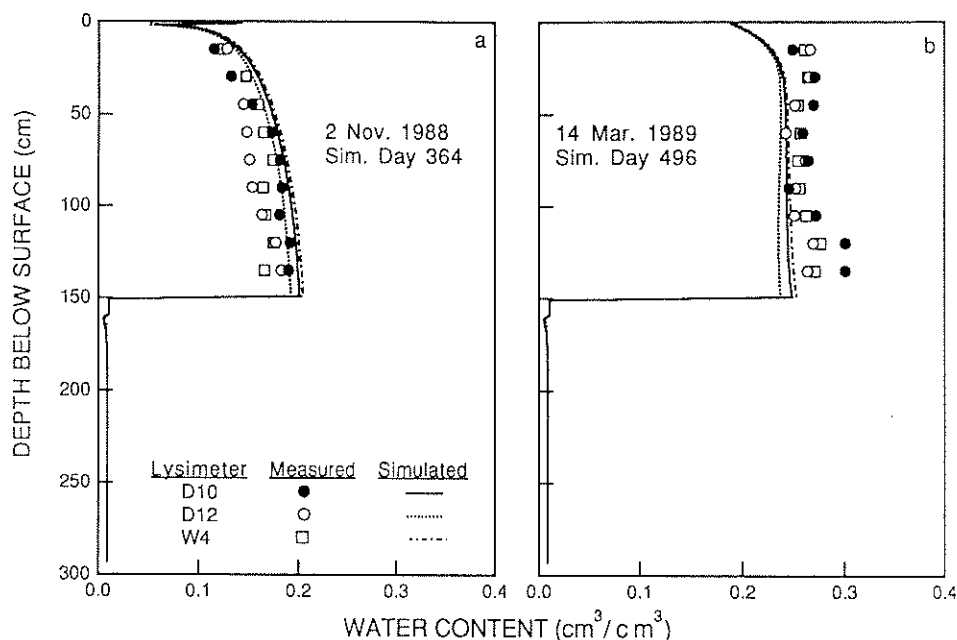


Fig. 8. Measured and simulated water contents for the 2 \times -average precipitation treatment on (a) 2 Nov. 1988 and (b) 14 Mar. 1989.

cm from the original simulation (Fig. 9). In separate simulations, the values of K_L and K_{vh} were individually adjusted within the entire silt loam layer according to the mean air temperature for each day. For K_L , we used the standard viscosity correction that Hopmans and Dane (1986) determined to be appropriate for soil. For K_{vh} , we made the ρ_{vs} and RH terms in Eq. [8] functions of the air temperature. Both K_L and K_{vh} changes resulted in storage differences of <0.1 cm from the original simulation. Although diurnal temperature changes were not represented, the results (using daily temperatures) suggest that their effect on K_L and K_{vh} would not significantly affect the simulation results. The effects of temperature changes on water retention and the movement of vapor (see the temperature-dependent term in Eq. [4]) were not evaluated.

Sensitivity tests that indicated important effects in-

volved variations in K_s and ℓ , the presence of a snow cover, and a reduction in PE. The effects of each change are described below.

Saturated Conductivity

During the curve-fitting process for the silt loam, 95% confidence intervals for the fitted value of K_s were generated using the RETC program (van Genuchten, 1985). The values encompassing the lower and upper intervals are 2.16 and 5.76 cm/h, respectively, or approximately 1.8 cm/h about the mean value. In terms of K_s , these values represent $0.54K_s$ and $1.43K_s$, respectively. The results in Fig. 10a show that the value of $0.54K_s$ allowed for increased storage (i.e., reduced evaporation) during all months; the value of $1.43K_s$ allowed for decreased storage (i.e., increased evaporation) during all months.

Pore Interaction Term

Having no measured values of K_L under dry conditions to guide the selection of an appropriate value for ℓ , we decided to explore the effect of a value of zero, i.e., no pore interaction. In Fig. 2 of Mualem (1976a), an ℓ (n in Mualem, 1976a) value of zero was nearly as valid as the value of 0.5 reported to be the best average value for a variety of soils. A lower value of ℓ yields a higher value of K_L (progressively more so as the soil dries), which increases evaporation. Thus, with $\ell = 0$, simulated storage decreased (i.e., evaporation increased) by 2.5 cm during the period from late spring to early fall of 1988 but did not change appreciably during the two winters (Fig. 10b). The reason for the seasonal effect is that the winter water contents were sufficiently high that K_L values were minimally affected by the change in ℓ . In contrast, in the summer, water contents were sufficiently low that K_L was significantly affected by the change in ℓ .

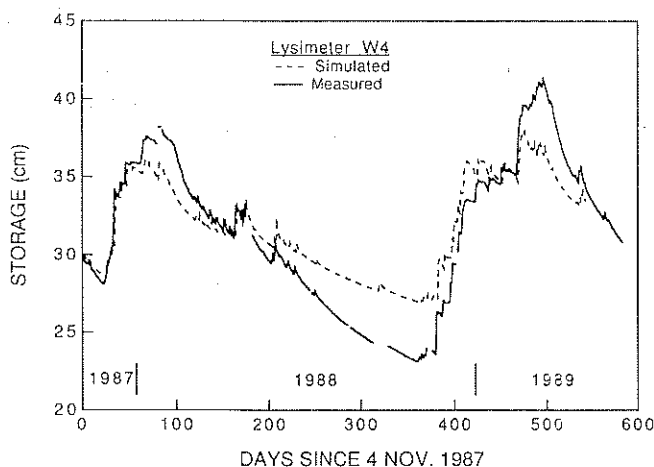


Fig. 9. Measured and simulated storage for the 2 \times -average precipitation treatment, lysimeter W4.

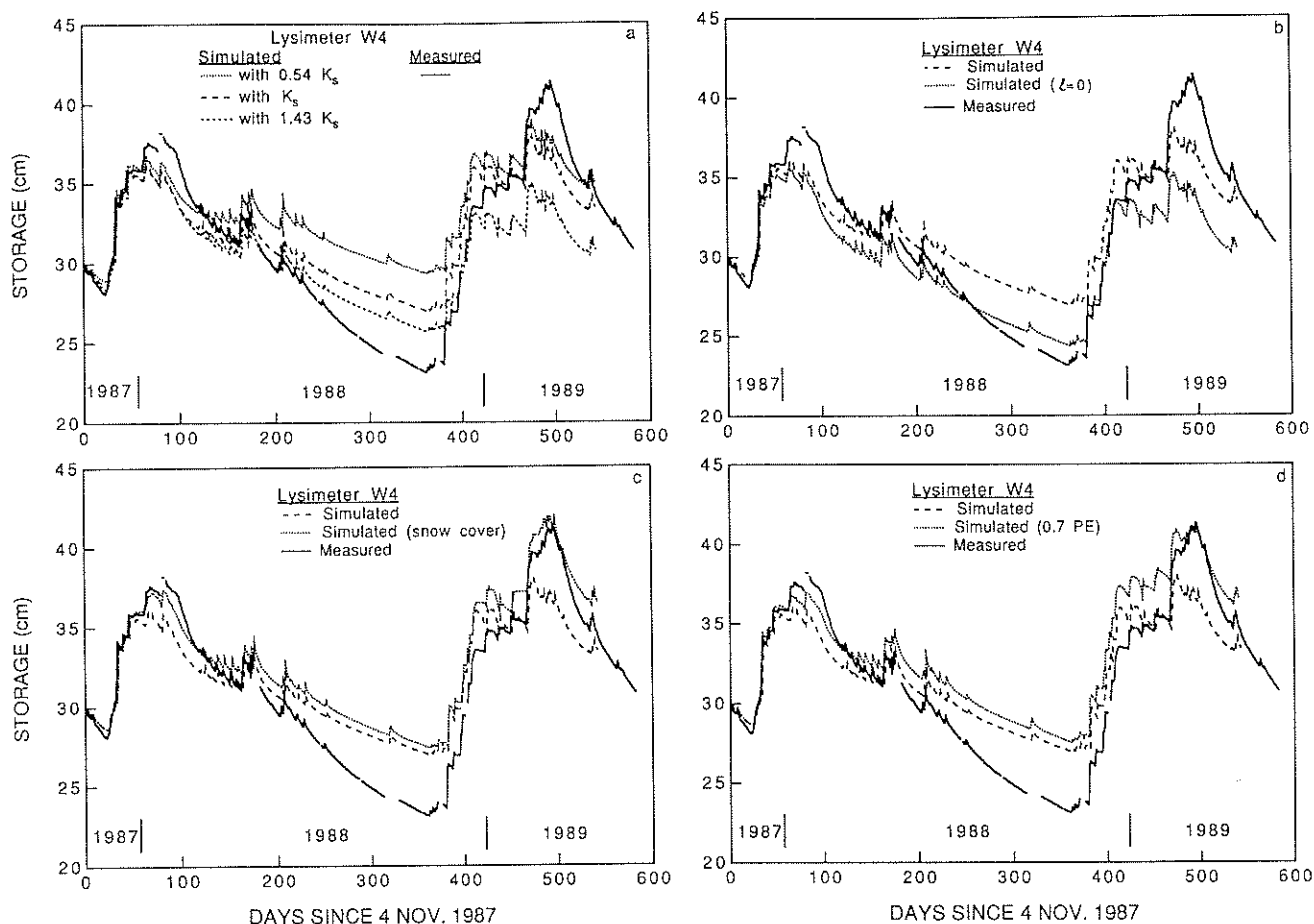


Fig. 10. Measured and simulated storage for the $2\times$ -average precipitation treatment, lysimeter W4, showing the effects of (a) 95% confidence intervals for saturated conductivity, K_s , (b) the pore interaction term, $\ell = 0$, (c) snow cover, and (d) 0.7 times the potential evaporation (PE).

Snow Cover

During each winter, a snow cover persisted for several weeks (Table 3). During that time, the model simulated more evaporation than was measured. The high albedo of snow can significantly reduce PE. In addition to the snow cover, average daily soil temperatures measured with thermocouples in lysimeters W2 and W4 indicated that the 0°C isotherm reached the 10-cm depth during the 1987–1988 winter and the 50-cm depth during the 1988–1989 winter. Frozen soil impedes evaporation by reducing water flow to the evaporative surface from below and by reducing the vapor density at the surface, thus lower the gradient that drives evaporation.

Although not explicitly included in the model, a snow cover was approximated by setting $\text{PE} = 0$ for the snow-cover periods in Table 3 (the effect of soil freezing could have been roughly approximated in the same manner). This reduction in PE amounted to 6.3 cm, which represents about 3% of the total PE for the simulation. Sublimation and the redistribution of water in response to soil freezing were assumed to be negligible. The results in Fig. 10c show that storage increased 2.0 cm in the first winter and 5.0 cm in the second winter relative to the original simulation (Fig. 9). The effects of the increased storage in winter persisted through the summer in the form of slightly higher

storage, on the order of 0.5 cm. A similar response was noted for simulations of lysimeter W2.

Potential Evaporation

Knowing that the model was overpredicting evaporation in the winter, particularly when air temperatures were $\leq 0^\circ\text{C}$ (Table 3), and that the Penman equation in Doorenbos and Pruitt (1977) has not been tested at the Hanford Site, we elected to reduce PE by 30% (i.e., 0.7PE). The lower PE resulted in less simulated evaporation in the months from late fall to early spring (Fig. 10d). Very little difference in evaporation was observed during the period from late spring to early fall. Subsequent review of the results showed that evaporation during these times was rarely at the PE rate, whereas the winter evaporation rates were often at PE rates, thus explaining why reduced PE improved the correspondence with measurements during winter. Replacing the PE concept with a direct simulation of both water and heat flow might resolve some of the discrepancies between predicted and measured evaporation rates.

Example Calibration

To demonstrate the potential for calibrating the model to match the data, we conducted a final simulation of lysimeter W4 using $1.43K_s$, ℓ equal to zero, a snow

Table 3. Periods of extended snow cover and mean daily air temperature equal to or below 0 °C.

Snow cover			Mean air temperature equal to or below 0 °C		
Simulation days	Starting date	Ending date	Simulation days	Starting date	Ending date
42 to 72	16 Dec. 1987	15 Jan. 1988	39 to 68	13 Dec. 1987	10 Jan. 1988
411 to 422	19 Dec. 1988	30 Dec. 1988	408 to 420	16 Dec. 1988	28 Dec. 1988
455 to 488	1 Feb. 1989	6 Mar. 1989	455 to 466	1 Feb. 1989	12 Feb. 1989

cover, and 0.7PE. The result in Fig. 11 shows that the model can be calibrated to significantly improve the match with the measured storage values. The root-mean-square error was 0.81 cm, which represents a 63% reduction from the original simulation in Fig. 9.

Breakthrough Treatment

Simulations using the silt loam desorption curve produced higher water contents at the 30-cm depth and lower water contents (by as much as 0.089 cm³/cm³) at the 135-cm depth than measured (Fig. 12). By 30 June 1988, the suction head at the sand-gravel interface had been lowered to 64 cm, a value at which a significant flux (i.e., 0.05 cm/yr) cannot enter the gravel. Given the high suction at the interface, these simulations with the desorption curve produced no drainage from the lysimeters.

The simulations were repeated using the silt loam sorption curve, assuming that this curve better represented the soil water status during the period after lysimeters were covered on 14 Mar. 1988 and wetted to breakthrough. Prior to being covered, these lysimeters were subjected to precipitation and evaporation that probably caused the water status in the silt loam to cycle along scanning curves between the main wetting and drying curves. For this series of simulations, however, the silt loam was assumed to be on the sorption branch only. The results were intended to demonstrate the importance of hysteresis in soil water retention to modeling of the protective barrier.

Simulations with the sorption curve produced water-content profiles that were in slightly better agreement with the measurements on 18 May 1988 than the simulations with the desorption curve (Fig. 12a). The maximum difference from the measurements on that date was 0.061 cm³/cm³ at the 135-cm depth. On 29 June 1988, the simulated water contents were all less than measured (and less than those simulated with the desorption curve), with the maximum difference from the measurements again being 0.061 cm³/cm³ at the 135-cm depth. Dane and Wierenga (1975) reported comparable results when using either sorption or desorption curves and no scanning curves (i.e., no hysteresis).

In the simulations, the onset of significant water movement (i.e., >0.05 cm/yr) into the sand layer occurred around Day 168 (20 Apr. 1988) when suction heads at the silt loam-sand interface decreased below 260 cm. Storage in the 0- to 165-cm depth range (equivalent to the depth of the weighing lysimeters) was 40.0 cm at this time. The onset of significant water movement into the gravel layer occurred around Day 186 (8 May 1988) when suction heads at the

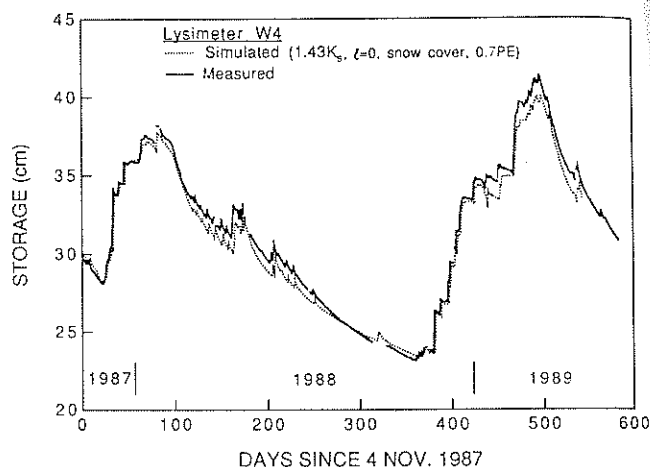


Fig. 11. Measured and simulated storage for the 2×-average precipitation treatment, lysimeter W4. Shown is the simulation with 1.43 times the saturated conductivity (K_s), the pore interaction term, $\ell = 0$, a snow cover, and 0.7 times potential evaporation (PE).

350 cm → fluid capillary

sand-gravel interface decreased below 60 cm. Storage in the 0- to 165-cm depth range was 43.9 cm at this time. Toward the end of the simulations, when drainage was occurring, the suction heads at the silt loam-sand and sand-gravel interfaces were approximately 13 and 3 cm, respectively. The measurements of suction head at the silt loam-sand interface ranged between 2 and 8 cm during the same period.

The results of a 239-d simulation show that simulated drainage appeared 11 to 12 d after measured drainage (Fig. 13). The measured-drainage values were 1.15 and 0.62 cm from lysimeters D9 and D11, respectively, on 28 June 1988. The corresponding simulated drainages using the sorption curve for the silt loam were 1.51 and 1.31 cm.

The sensitivity of simulated drainage to uncertainty in the value of K_{fs} was evaluated using variations of 1.8 cm/h about the K_{fs} value. This variation represented the size of the confidence interval calculated during curve fitting of the laboratory desorption data. Although not based on field data, the variation is sufficient to demonstrate sensitivity. The results showed that using $1.56K_{fs}$ for the silt loam caused drainage to occur 3 d early than when using K_{fs} . In contrast, using $0.56K_{fs}$ delayed the start of drainage by 11 d in lysimeter D9 and resulted in no drainage from lysimeter D11 (although, if the simulations were continued 1 to 2 d more, drainage would probably have occurred). Using $1.56K_{fs}$, the simulated drainage values from lysimeters D9 and D11 were 1.98 and 1.77 cm, respectively. Using $0.56K_{fs}$, the simulated drainage val-

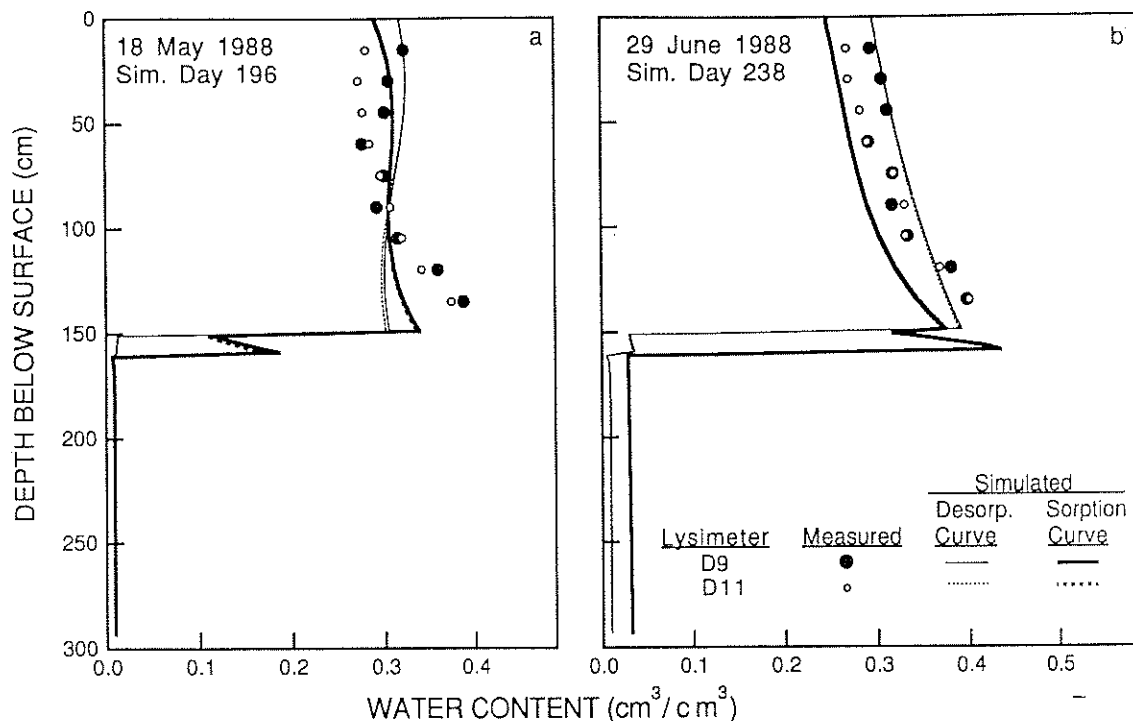


Fig. 12. Measured and simulated water contents for the breakthrough treatment on (a) 18 May 1988 and (b) 29 June 1988.

ues were zero. For the two lysimeters, the simulated drainage values bracket the measured values. These results demonstrate the sensitivity of cumulative drainage to just one soil hydraulic parameter.

CONCLUSIONS

Without any calibration to field data, the UNSAT-H model reproduced much of the water-balance changes that were observed in the field. Differences between measured and simulated values of water content and storage were largest in winter (when evaporation was

overpredicted) and summer (when evaporation was underpredicted). Sensitivity tests demonstrated the importance of the hydraulic-conductivity function (specifically, K_s and θ), snow cover, and the calculation of potential evaporation to successful modeling of storage in a protective barrier. When these parameters and processes were adjusted (though not optimized), the root-mean-square error for the $2 \times$ -average treatment was reduced by 63%. This result suggests that a more rigorous calibration in the future will probably reduce the error further.

For the breakthrough treatment, simulated drainage was obtained only by using field-measured sorption and saturated-conductivity data. This result demonstrates that hysteresis is important to successful modeling of drainage through protective barriers.

The results presented here show how the uncalibrated model performed and indicates areas for model improvement. Subsequent work will be focused on unsaturated-conductivity measurements at suction-head values well above 200 cm of water, hysteresis, snow cover, frozen soil, the calculation of potential evaporation, and the effects of temperature variations on water and vapor flow. This work will include long-term comparisons such as presented here as well as short-term comparisons using hourly data from the weighing lysimeters. Once all major processes operating within the barrier are identified and incorporated, parameters used to simulate the protective barrier will be optimized by calibrating with a subset of the available lysimeter data. We believe that additional measurements, model enhancements, and calibration can lead to the successful prediction of drainage rates as low as 0.05 cm/yr through layered soil in a semiarid climate.

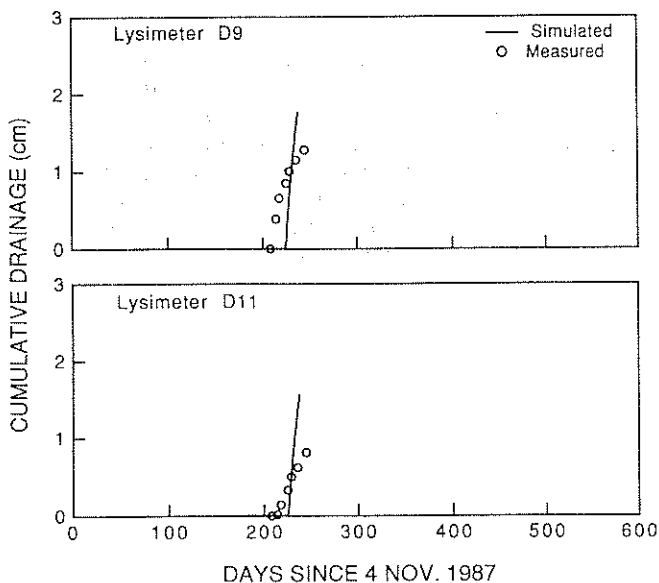


Fig. 13. Measured and simulated drainage for the breakthrough treatment using the silt loam sorption curve.

ACKNOWLEDGMENTS

The authors gratefully acknowledge the efforts of Pacific Northwest Laboratory and Westinghouse Hanford Company employees who have participated in the design, construction, and monitoring of the Field Lysimeter Test Facility.

REFERENCES

- Dane, J.H., and P.J. Wierenga. 1975. Effect of hysteresis on the prediction of infiltration, redistribution and drainage of water in a layered soil. *J. Hydrol. (Amsterdam)* 25:229-242.
- Doorenbos, J., and W.O. Pruitt. 1977. Guidelines for predicting crop water requirements. FAO Irrig. Pap. no. 24. 2nd ed. FAO, Rome.
- Fayer, M.J., W. Conbere, R.R. Heller, and G.W. Gee. 1985. Model assessment of protective barrier designs. Publ. PNL-5604. Pac. Northwest Lab., Richland, WA.
- Fayer, M.J., and T.L. Jones. 1990. UNSAT-H Version 2.0: Unsaturated soil water and heat flow model. Publ. PNL-6779. Pac. Northwest Lab., Richland, WA.
- Gee, G.W., R.R. Kirkham, J.L. Downs, and M.D. Campbell. 1989. The Field Lysimeter Test Facility (FLTF) at the Hanford Site: Installation and initial tests. Publ. PNL-6810. Pac. Northwest Lab., Richland, WA.
- Gupta, S.K., K.K. Tanji, D.R. Nielsen, J.W. Biggar, C.S. Simmons, and J.L. MacIntyre. 1978. Field simulation of soil-water movement with crop water extraction. *Water Sci. Eng. Pap.* no. 4013. Dep. of Land, Air, and Water Resour., Univ. of California, Davis.
- Hillel, D. 1980. Fundamentals of soil physics. Academic Press, New York.
- Hopmans, J.W., and J.H. Dane. 1986. Temperature dependence of soil hydraulic properties. *Soil Sci. Soc. Am. J.* 50:4-9.
- Horton, R. 1989. Canopy shading effects on soil heat and water flow. *Soil Sci. Soc. Am. J.* 53:669-679.
- Klute, A., and C. Dirksen. 1986. Hydraulic conductivity and diffusivity: Laboratory methods. p. 687-734. *In* A. Klute (ed.) *Methods of soil analysis. Part 1.* 2nd ed. Agron. Monogr. 9. ASA and SSSA, Madison, WI.
- Lascano, R.J., C.H.M. van Bavel, J.L. Hatfield, and D.R. Upchurch. 1987. Energy and water balance of a sparse crop: Simulated and measured soil and crop evaporation. *Soil Sci. Soc. Am. J.* 51:1113-1121.
- Miller, D. 1971. Water retention and flow in layered soil profiles. p. 107-117. *In* R.R. Bruce (chair) *Field soil water regime.* SSSA Spec. Publ. 5. SSSA, Madison, WI.
- Miller, D., and W.C. Bunger. 1963. Moisture retention by soil with coarse layers in the profile. *Soil Sci. Soc. Am. Proc.* 27: 586-589.
- Mualem, Y. 1976a. A new model for predicting the hydraulic conductivity of unsaturated porous media. *Water Resour. Res.* 12:513-522.
- Mualem, Y. 1976b. A catalogue of the hydraulic properties of soils. Res. Progr. Rep. no. 442. Technion, Israel Inst. of Technol., Haifa.
- Nimah, M.N., and R.J. Hanks. 1973. Model for estimating soil water, plant, and atmospheric interrelations: I. Description and sensitivity. *Soil Sci. Soc. Am. Proc.* 37:522-527.
- Rockhold, M.L., M.J. Fayer, and G.W. Gee. 1988. Characterization of unsaturated hydraulic conductivity at the Hanford Site. Publ. PNL-6488. Pac. Northwest Lab., Richland, WA.
- Sellers, P.J., and J.L. Dorman. 1987. Testing the simple biosphere model (SiB) using point micrometeorological and biophysical data. *J. Clim. Appl. Meteor.* 26:622-651.
- Simmons, C.S., and G.W. Gee. 1981. Simulation of water flow and retention in earthen cover materials overlying uranium mill tailings. Publ. PNL-3877. Pac. Northwest Lab., Richland, WA.
- Stone, W.A., J.M. Thorp, O.P. Gifford, and D.J. Houtink. 1983. Climatological summary for the Hanford area. Publ. PNL-4622. Pac. Northwest Lab., Richland, WA.
- U.S. Department of Energy. 1987. Final environmental impact statement disposal of Hanford defense high-level, transuranic and tank wastes, Hanford Site, Richland, Washington. DOE/EIS-0113 (Vol. 3). U.S. Dep. of Energy, Washington, DC.
- van Genuchten, M.Th. 1978. Calculating the unsaturated hydraulic conductivity with a new closed-form analytical model. Publ. 78-WR-08. Dep. of Civil Eng., Princeton Univ., Princeton, NJ.
- van Genuchten, M.Th. 1985. RETC.F77: A program to analyze observed soil water tension and hydraulic conductivity data. U.S. Salinity Lab. Spec. Rep. U.S. Salinity Lab., Riverside, CA.
- Wang, H.F., and M.P. Anderson. 1982. Introduction to groundwater modeling. W.H. Freeman and Co., San Francisco.
- Witono, H., and L. Bruckler. 1989. Use of remotely sensed soil moisture content as boundary conditions in soil-atmosphere water transport modeling 1. Field validation of a water flow model. *Water Resour. Res.* 25:2423-2435.

Imp. paper
gives the
details
f
cap.
10°C.

Editorial Board, SSSA

ROBERT J. LUXMOORE, editor-in-chief

Technical Editors

J.M. BIGHAM (Div. S-5, S-9) J.H. DANE (Div. S-1)
D.K. CASSEL (Div. S-6) M.S. SMITH (Div. S-3, S-7)
N.W. CHRISTENSEN (Div. S-4, S-8) D.L. SPARKS (Div. S-2)

Associate Editors

L.R. AHUJA R.H. LOEPPERT
M.M. ALLEY K. MCSWEENEY
M.C. AMACHER R.L. MIKKELSEN
A. AMOZEGAR D. MULLA
S.H. ANDERSON D.D. MYROLD
J.S. ANGLE W.D. NETTLETON
J.R. BOYLE C.G. OLSON
J.A. BURGER T.B. PARKIN
W.J. BUSSCHER D.E. RADCLIFFE
E.J. DIEBERT G.W. REHM
T.A. DOERGE M.J.M. ROMKENS
L.R. DREES D.G. SCHULZE
W.W. FRYE A.P. SCHWAB
R.C. GRAHAM N.E. SNECK
D.F. GRIGAL S.J. SMITH
R.D. HARTER J.L. STARR
R.L. HILL D.L. SUAREZ
P.M. HUANG M.A. TABATABAI
G.L. HUTCHINSON R.F. TURCO
P.M. JARDINE D.R. UPCHURCH
D.B. JAYNES M.J. VEPKASKAS
R.G. KACHANOSKI D.T. WESTERMANN
J.M. KELLY R.S. YOST

WILLIAM R. LUELLEN, managing editor
R.F. BARNES, executive vice president
D.M. KRAL, associate executive vice president

PAMM KASPER, associate production editor
MARIAN K. VINNEY, assistant editor

Published bimonthly by the Soil Science Society of America, Inc. Second-class postage paid at Madison, WI, and at additional mailing offices. Business and editorial office at 677 S. Segoe Rd., Madison, WI 53711 USA.

Subscription rates (nonmember): \$85 per year, postpaid within the USA; all others \$94.50. Single copies, \$16 USA; elsewhere, \$18. New subscriptions, renewals, and new memberships that include the SSSA Journal begin with the first issue of the current year. Claims for copies lost in the mail must be received within 90 days of publication date for domestic subscribers, and within 26 weeks of publication date for foreign subscribers. Send orders to the Business Manager.

At least one author of each unsolicited paper submitted to the SSSA Journal must be an active, emeritus, sustaining member representative, graduate student, or dues-paying undergraduate student member of the Soil Science Society of America, Crop Science Society of America, or American Society of Agronomy. Articles must be approved by the Editorial Board.

Contributions to the SSSA Journal may be (i) papers and notes on original research; and (ii) "Comments and Letters to the Editor" containing (a) critical comments on papers published in one of the Society outlets or elsewhere, (b) editorial comment or comments by Society officers, or (c) personal comments on matters having to do with soil science. Letters to the Editor are limited to one printed page. Contributions need not have been presented at annual meetings. Original research findings are interpreted to mean the outcome of scholarly inquiry, investigation, or experimentation having as an objective the revision of existing concepts, the development of new concepts, or the development of new or improved techniques in some phase of soil science. Short, critical reviews or essays on timely subjects, upon invitation by the Editorial Board, may be published on a limited basis. Refer to SSSA Publication Policy (Soil Sci. Soc. Am. J. 55(1):1-2, 1991) and to the Publications Handbook and Style Manual (ASA-CSSA-SSSA, 1988).

Manuscripts are to be sent to Dr. Robert J. Luxmoore editor-in-chief, SSSA, Oak Ridge National Lab, P.O. Box 20008, Bldg. 1505, Oak Ridge, TN 37831-6038 (Phone: 615-574-7357). Four copies of the manuscript, on line-numbered paper, are required. All other correspondence should be directed to the Managing Editor, 677 S. Segoe Rd., Madison, WI 53711.

Volunteered papers will be assessed a charge of \$40 per page for each printed page from page one through page four; a charge of \$190 per page (\$95 per half page) will be assessed for additional pages. No charge will be assessed against invited review papers or comments and letters to the editor. The Society absorbs the cost of reproducing illustrations up to \$15 for each paper.

Trade names are sometimes listed in papers published in this journal. No endorsement of these products by the publisher is intended, nor is any criticism implied of similar products not mentioned.

Copyright © 1992 by the Soil Science Society of America, Inc. Permission for printing and for reprinting the material contained herein has been obtained by the publisher. Other users should request permission from the author(s) and notify the publisher if the "fair use" provision of the U.S. Copyright Law of 1976 (P.L. 94-553) is to be exceeded.

1992 OFFICERS OF SSSA

W. W. McFEE, Purdue University, West Lafayette, IN, president
DARRELL W. NELSON, University of Nebraska, Lincoln, NE, president-elect
F. P. MILLER, Ohio State University, Columbus, OH, president
R. F. BARNES, ASA-CSSA-SSSA Headquarters, Madison, WI, executive vice president

Soil Science Society of America JOURNAL

VOL. 56

May-June 1992

No. 3

CONTENTS

Page

Division S-1—Soil Physics

- Moment Method Applied to Solute Transport with Binary and Ternary Exchange...
..... Feike J. Leij and J.H. Dane 667
- Infiltration Simulations among Five Hydraulic Property Models...
..... Sam Alessi, Lyle Prunty, and W.M. Schuh 675
- Coupled Diffusion of Exchangeable Cations in Soil...
..... Dean Rhue 683
- Hydrologic Modeling of Protective Barriers: Comparison of Field Data and Simulation Results...
..... M.J. Fayer, M.L. Rockhold, and M.D. Campbell 690
- Fiberglass Wicks for Sampling of Water and Solutes in the Vadose Zone...
..... J. Boll, T.S. Steenhuis, and J.S. Selker 701
- Thermally Driven Water and Octane Redistribution in Unsaturated, Closed Soil Cells...
..... Lyle Prunty 707
- Macropore and Surface Seal Interactions Affecting Water Infiltration into Soil...
..... S.D. Ela, S.C. Gupta, and W.J. Rawls 714
- Bypass Water Flow through Unsaturated Microaggregated Tropical Soils...
..... R. Radulovich, P. Sollins, P. Baveye, and E. Solórzano 721
- Microrelief and Rainfall Effects on Water and Solute Movement in Earthworm Burrows...
..... M.D. Trojan and D.R. Linden 727
- In Situ Measurement of the Effective Transport Volume for Solute Moving through Soil...
..... B.E. Clothier, M.B. Kirkham, and J.E. McLean 733

Division S-2—Soil Chemistry

- Effect of Sorption on the Biodegradation of Quinoline...
..... S.C. Smith, C.C. Ainsworth, S.J. Traina, and R.J. Hicks 737
- Significance of Soil Chemical Heterogeneity for Spatial Behavior of Cadmium in Field Soils...
..... Alexandra E. Boekhold and Sjoerd E.A.T.M. Van der Zee 747
- Changes in Aluminum and Phosphorus Solubilities in Response to Long-Term Fertilization...
..... J.A. Hetrick and A.P. Schwab 755
- Partitioning Dissolved Inorganic and Organic Phosphorus Using Acidified Molybdate and Isobutanol...
..... K. Jayachandran, A.P. Schwab, and B.A.D. Hetrick 758
- ERRATUM... 765

Division S-3—Soil Microbiology & Biochemistry

- Nitric Oxide and Nitrous Oxide Production from Soil: Water and Oxygen Effects...
..... C.F. Drury, D.J. McKenney, and W.I. Findlay 766
- Landscape-Scale Variations in Denitrification...
..... D.J. Pennock, C. van Kessel, R.E. Farrell, and R.A. Sutherland 770
- Particulate Soil Organic-Matter Changes across a Grassland Cultivation Sequence...
..... C.A. Cambardella and E.T. Elliott 777
- Crop Rotation and Residue Management Effects on Soil Carbon and Microbial Dynamics...
..... H.P. Collins, P.E. Rasmussen, and C.L. Douglas, Jr. 783
- Grain Sorghum-Soybean Rotation and Fertilization Influence on Vesicular-Arbuscular Mycorrhizal Fungi...
..... J.R. Ellis, W. Roder, and S.C. Mason 789
- New Formulae for Mass Spectrometric Analysis of Nitrous Oxide and Dinitrogen Emissions...
..... J.R.M. Arah 795

Division S-4—Soil Fertility & Plant Nutrition

- State-Space Approach to Spatial Variability of Crop Yield...
..... Ole Wendroth, A.M. Al-Omran, C. Kirda, K. Reichardt, and D.R. Nielsen 801
- Ameliorating Chlorosis-Inducing Soils with Rock Materials of Varying Porosity and Iron Content...
..... Gerhard Clemens and Arie Singer 807
- Determination of Bioavailable Phosphorus in Soil...
..... S.J. Thien and R. Myers 814
- Maize Root Distribution between Phosphorus-Fertilized and Unfertilized Soil...
..... Jiancai Zhang and S.A. Barber 819
- Cotton Response to Residual Fertilizer Potassium on Vermiculitic Soil: Organic Matter and Sodium Effects...
..... K.G. Cassman, B.A. Roberts, and D.C. Bryant 823
- Role for Potassium in the Iron-Stress Response Mechanism of Iron-Efficient Oat...
..... D.F. Hughes, V.D. Jolley, and J.C. Brown 830